

RESEARCH

Open Access

# Structural, electrical, and decorative properties of sputtered zirconium thin films during post-annealing process

Kaykhosrow Khojier<sup>1\*</sup>, Hadi Savaloni<sup>2</sup> and Fatemeh Jafari<sup>3</sup>

## Abstract

Zirconium thin films were deposited on a glass substrate using direct current magnetron sputtering technique and then post-annealed at different temperatures (100°C to 500°C in steps of 100°C) in an oxygen constant flow. The dependence of crystallographic structure, surface morphology, chemical composition, and electrical and decorative properties of the films on the annealing temperature was investigated. X-ray diffraction showed different phases of zirconium oxide at different annealing temperatures. It is observed that crystallite size and nanostrain increase with annealing temperature. Atomic force microscopy results showed granular structure in all samples, while both grain size and film surface roughness increased with the annealing temperature. Energy dispersive X-ray analysis data showed that the ratio of O/Zr was approximately 1.6, 1.7, 1.9, 2.1, and 2.2 at annealing temperatures of 100°C, 200°C, 300°C, 400°C, and 500°C, respectively. The annealed films at higher temperatures (400°C and 500°C) were transparent, while annealed films at lower temperatures (100°C to 300°C) were grey and brown, respectively. The variation of electrical resistance of samples with applied voltage was approximately constant, while it increased with annealing temperature.

**Keywords:** Thin films; ZrO<sub>x</sub>; Crystallographic structure; Morphology; Electrical resistance; Decorative properties

## Background

The study of metal oxides, especially in the form of thin films, has both scientific and technological significance. Zirconia (ZrO<sub>2</sub>) is one of these materials that exhibit remarkable properties. Because of its desirable physical and chemical properties, such as high melting point (2,700°C), low thermal conductivity (4.2 W m<sup>-1</sup> K<sup>-1</sup> at room temperature) [1], high hardness (18 GPa for monoclinic phase and 14 to 11 GPa for amorphous [2,3]), excellent chemical and corrosion resistance [2,4], high refractive index (2.2), large band gap (5 eV), high transparency in the visible and near-IR region [5], high dielectric constant (approximately 25 [6]), and biocompatibility [7], it is widely used in coating materials against corrosion, wear and oxidation, electronic devices, high refractive mirrors, broadband interference filters, decorative devices, active electro-optical devices, and anti-reflection coatings in optical industries [6,8-12]. Furthermore, because of its

color (similar to tooth color), biocompatibility, and adequate mechanical properties, zirconia is widely used in dentistry [13].

Among various physical and chemical methods for preparation of zirconium oxide thin films [14-22], post-annealing of zirconium layers is a simple, low-cost, suitable, and flexible method. In this technique, variation of annealing conditions including annealing temperature, time, and environment results in different nanostructures with interesting properties. Some researchers have also used post-annealing of Zr or ZrO<sub>2</sub> layers for preparation of zirconia thin films with new and different properties [23-25].

In this paper, in order to more deeply understand the post-annealing effect on the Zr thin films, we have performed the post-annealing procedure on sputter-coated Zr/glass thin films with constant flow of oxygen at different temperatures and investigated the effect of this process on the crystallographic structure, surface morphology, chemical composition, and decorative and electrical properties of the produced zirconium oxide thin films.

\* Correspondence: khojier@iauc.ac.ir

<sup>1</sup>Department of Physics, Chalous Branch, Islamic Azad University, Chalous, Iran

Full list of author information is available at the end of the article

## Experimental details

Zirconium thin films of 90-nm thickness were deposited by means of a direct current (DC) magnetron sputtering system using a circular sputtering target (99.998% purity) of 76-mm diameter and 1-mm thickness. The target-to-substrate distance was 10 cm. A continuously variable DC power supply of 600 V and 150 mA was used as a power source for sputtering. The thickness and deposition rate of Zr films were checked *in situ* using a quartz crystal monitor (6 MHz gold, INFICON Company, East Syracuse, NY, USA) located near the substrate during the sputtering process. The zirconium thin films were deposited with a deposition rate of 9 Å/s at room temperature. The base pressure was  $4 \times 10^{-5}$  mbar which changed to  $2.8 \times 10^{-3}$  mbar during deposition of Zr. The purity of argon gas in this work was 99.998% and controlled by a mass flow controller. The substrates for the deposition were  $20 \times 20$  mm<sup>2</sup> glass (cut from a microscope slide) and were cleaned with acetone and ethanol in an ultrasound cleaner for a few minutes. The surface roughness of the substrates was measured by a Talysurf profilometer (Taylor-Hobson, Leicester, UK). The root mean square (rms) substrate roughness was 0.3 nm. Post-annealing of Zr/glass films was performed using a tube furnace at five different temperatures (100°C to 500°C in steps of 100°C) with a 200 sccm (standard cubic centimeter per minute) flow of oxygen (purity of 99.98%). The samples reached the selected temperature with a thermal gradient of 5°/min and were kept at the annealing temperature for 60 min, then gradually cooled down to room temperature. The flow rate of oxygen gas was controlled by a mass flow controller. Nanostructure and crystallographic orientation of the samples were obtained using a Philips XRD X'pert MPD diffractometer (Cu K $\alpha$  radiation, 40 kV and 30 mA; FEI Co., Hillsboro, OR, USA) with a step size of 0.02° and count time of 1 s per step. A field emission scanning electron microscope (model: MV2300, CamScan, Czech and England) and an atomic force microscope (AFM; Auto Probe PC, Park Scientific Instrument, Santa Clara, CA, USA) were also employed for investigation of chemical composition and surface morphology of the samples, respectively. The electrical resistance of the films was also measured by a two-probe instrument with an excitation wavelength at 320 nm. The excitation wavelength in UV range was needed due to the high dielectric constant (approximately 25 [6]) of zirconium oxide, so that the electrical resistance measurement of samples without the UV excitation wavelength was impossible.

## Results and discussion

### Crystallographic structure

Zirconium oxide exists in different crystalline phases, namely amorphous [26,27], cubic [28,29], monoclinic [28,30], tetragonal [31,32], orthorhombic [33,34], and

combination of different phases [24]. All these structures are strongly affected by the preparation method and growth parameters. X-ray diffraction patterns of Zr/glass thin films annealed at different temperatures for 60 min are shown in Figure 1, while the numerical data of this analysis are given in columns 3 and 4 of Table 1. The X-ray diffraction (XRD) pattern of an annealed sample at 100°C shows two peaks at 31.89° and 36.53° that can be related to the ZrO<sub>2</sub>(012) diffraction line of orthorhombic phase (with reference to JCPDS card no. 33-1483,  $2\theta$ : 31.889°) and Zr(101) diffraction line (with reference to JCPDS card no. 05-0665,  $2\theta$ : 36.510°). At 200°C annealing temperature, the intensity of the zirconium peak is decreased, while the ZrO<sub>2</sub>(012) peak intensity is increased. By increasing the annealing temperature to 300°C, the abovementioned peaks disappeared and three new peaks appeared at 28.05°, 29.81°, and 34.21° diffraction angles. These peaks can be attributed to the ZrO<sub>2</sub>(111) crystallographic orientation of monoclinic phase (with reference to JCPDS card no. 05-0543,  $2\theta$ : 28.036°), ZrO<sub>2</sub>(101) crystallographic orientation of tetragonal phase (with reference to JCPDS card no. 24-1164,  $2\theta$ : 29.807°), and ZrO<sub>2</sub>(002) crystallographic orientation of monoclinic phase (with reference to JCPDS card no. 05-0543,  $2\theta$ : 34.195°), respectively. When the annealing temperature increased to the higher temperatures (i.e., 400°C and 500°C), only the intensities of these peaks are increased and no new

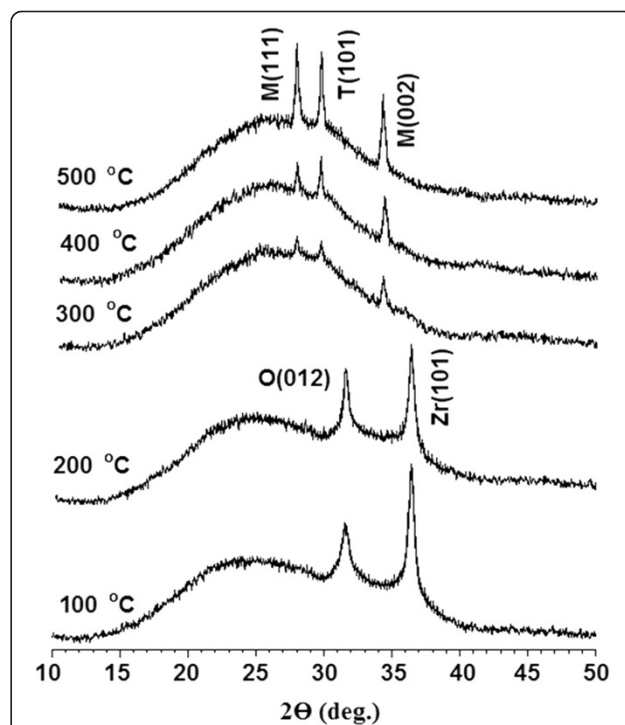


**Figure 1** X-ray diffraction patterns of zirconium thin films annealed at different temperatures with constant flow of oxygen.

**Table 1 Details of XRD and AFM analyses**

Sample		XRD analysis					AFM analysis		
Code	AT (°C)	2θ (deg.)	(hkl)	<i>d</i> (Å)	ε ×10 <sup>-5</sup>	<i>D</i> (nm)	<i>D</i> (nm)	rms	<i>R</i> <sub>ave</sub>
I	100	31.89	O(012)	2.80	-142	27	32	2.5	2.1
		36.53	Zr(101)	2.45	-366	28			
II	200	31.91	O(012)	2.80	-142	34	41	2.9	2.3
		36.53	Zr(101)	2.45	-366	32			
III	300	28.05	M(111)	3.17	-314	32	48	4.2	3.4
		29.81	T(101)	2.99	-166	30			
		34.21	M(002)	2.61	-381	28			
IV	400	28.07	M(111)	3.17	-314	62	78	6.8	7.8
		29.85	T(101)	2.99	-166	55			
		34.25	M(002)	2.61	-381	49			
V	500	28.09	M(111)	3.17	-314	74	102	7.6	10.8
		29.87	T(101)	2.98	-500	70			
		34.27	M(002)	2.61	-381	62			

AT annealing temperature, *D* crystallite/grain size, O orthorhombic, M monoclinic, T tetragonal, Zr zirconium.

peaks are observed. On the other hand, it may be suggested that by increasing the annealing temperature between 300°C and 500°C, little change may occur in the structure of ZrO<sub>2</sub> films.

In summary, the results of XRD analysis of the samples produced in this work show that one may distinguish two groups of nanostructures. Group I (samples I and II) includes the films annealed at lower temperatures (100°C and 200°C) with a complex structure of ZrO<sub>2</sub> (orthorhombic) and Zr (hexagonal). Group II (samples III to V) includes the films annealed at higher temperatures (300°C to 500°C) that were completely oxidized and showed a mixed crystallographic structure of monoclinic and tetragonal.

It can be seen in column 3 of Table 1 that the position of all diffraction lines is shifted to higher diffraction angles relative to that of the powder sample. Furthermore, the sample annealed at the highest annealing temperature shows a larger shift than those annealed at lower temperatures. The observed shifts provide information to calculate the nanostrain (ε) in the body of the film [35,36] using

$$\varepsilon = (d-d_0)/d_0, \quad (1)$$

where *d* is the plane spacing of the sample (column 5 of Table 1) and *d*<sub>0</sub> is the plane spacing of the standard powder sample. Variations of nanostrain for all diffraction lines are shown in column 6 of Table 1. The results for all samples show compressive strain. Considering the ZrO<sub>2</sub>(101) (i.e., T(101), tetragonal) diffraction line in the samples annealed at higher temperatures of 300°C to 500°C, it can be deduced that this compressive strain is increased to its highest value at 500°C. In general, the volume energy of

the thin film decreases with increasing of the substrate (annealing) temperature due to increased diffusion effect, which in turn reduces the nanostrain in the structure of the thin film [37]; at the same time by increasing the temperature, the contribution of the thermal strain on the total strain is increased, causing the strain to increase.

The competition between the diffusion process and thermal strain at different substrate (annealing) temperatures may have been the cause of the above observations in the nanostrain in zirconium oxide films reported in Table 1.

In order to obtain the crystallite size (coherently diffracting domains) of the samples, we used the Scherrer relation [38]

$$D = \frac{k\lambda}{B \cos\theta}, \quad (2)$$

where λ is the wavelength of X-ray, θ is the Bragg angle, and *k* is a dimensionless constant which is related to the shape and distribution of crystallites [39] (usually taken as unity). For obtaining the value of *B*, we used the usual procedure of full width at half maximum (FWHM) measurement technique [40]; therefore,

$$B = (W_0^2 - W_i^2)^{1/2}, \quad (3)$$

where *W*<sub>0</sub> is the FWHM of the sample and *W*<sub>*i*</sub> is the FWHM of the stress-free sample (standard SiO<sub>2</sub> single-crystal sample). The calculated crystallite size *D* (coherently diffracting domains) obtained from the above procedure is given in column 7 of Table 1. This result shows that the crystallite size in each group of films (i.e., groups I and II) increases with the annealing temperature.

This behavior may be due to the increased diffusion effect with annealing temperature. A similar effect is reported by Ciosek et al. [23].

### Surface morphology

3-D AFM images of selected zirconium oxide samples prepared in this work are shown in Figure 2, while grain size (obtained from 2-D AFM images by JMicrovision code) and surface roughness parameters of all samples are given in columns 8 to 10 of Table 1. The results show a granular structure for all samples, while grain size in each group of the samples (consistent with XRD results) and surface roughness increase with annealing temperature. This behavior is due to the high annealing temperature that provides energy of film atoms to enhance mobility. Increasing of mobility also increases the coalescence and produces larger grains with deeper valleys between them; hence, higher surface roughness is obtained. A similar behavior with annealing temperature is also obtained and reported in [41].

The grain sizes obtained from XRD data (27 to 74 nm) are smaller than the results obtained from AFM images (32 to 102 nm). These differences can be attributed to the fact that the AFM images show only surface of the grains.

### Chemical composition and color of the produced samples

In addition to other factors such as hardness, color of zirconia coatings is important in dentistry and decorative devices. For this reason, we have studied the dependence of color and chemical composition of samples on annealing temperature. The chemical composition deduced from energy dispersive X-ray (EDAX) measurements and colors of

the films produced in this work are given in Figure 3. These results indicate that the O/Zr ratio in the structure of the samples (i.e.,  $x$  in  $ZrO_x$ ) increases with the annealing temperature. The stoichiometry of the zirconium oxide thin films was found to be approximately 1.6, 1.7, 1.9, 2.1, and 2.2 at annealing temperatures of 100°C, 200°C, 300°C, 400°C, and 500°C, respectively. On the other hand, the result shows that the degree of film oxidation increases with annealing temperature. Koski et al. [42] have reported that zirconium oxide is colorless and transparent when it is fully oxidized. This color is due to the profusion of oxygen atoms in the lattice structure. The color is grey or brown when the O/Zr ratios are 1.6 and 1.8, respectively. A color of grey happens when the thin films are rich in metal. These results are consistent with the color of our samples in this work. Figure 4 shows the images of our samples annealed at 100°C, 300°C, and 500°C with grey, brown, and transparent (colorless) colors, respectively.

The results of EDAX analysis and color of samples are consistent with XRD patterns. The films annealed at lower temperatures (100°C and 200°C) due to the low influence of oxygen had a mixed structure of  $ZrO_2$  and Zr and were substoichiometric and grey, whereas the films annealed at higher temperatures (400°C and 500°C) due to the deeper/more influence of oxygen were completely oxidized, colorless, and overstoichiometric.

### Electrical resistance

The  $I$ - $V$  curve was measured to study the electrical behavior of the films. This work was done with a two-probe system equipped with a nano-ammeter with an excitation wavelength at 320 nm. Figures 5 and 6 show the variation

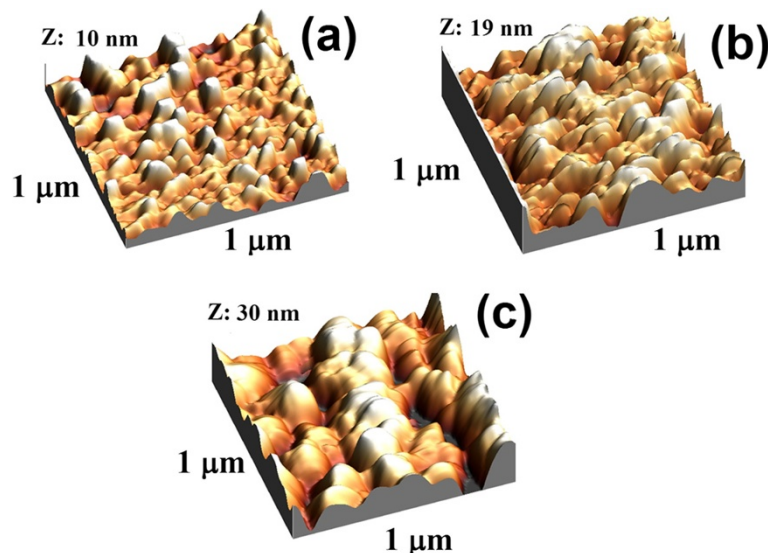
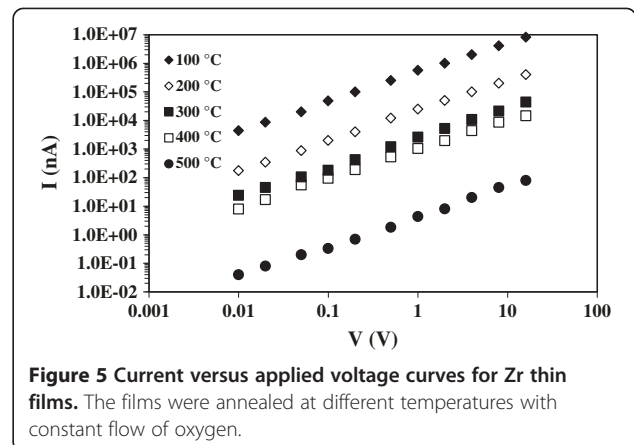
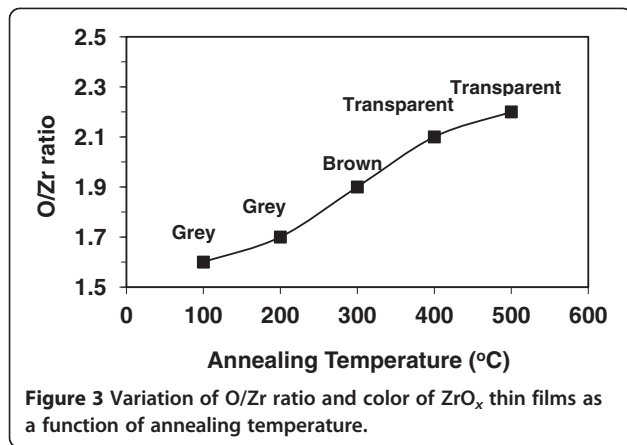


**Figure 2** 3-D AFM images of selected zirconium thin films. The films were annealed at (a) 100°C, (b) 300°C, and (c) 500°C temperatures with constant flow of oxygen.



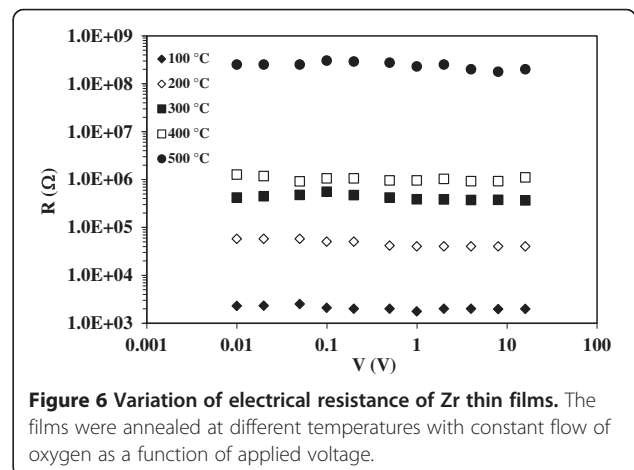
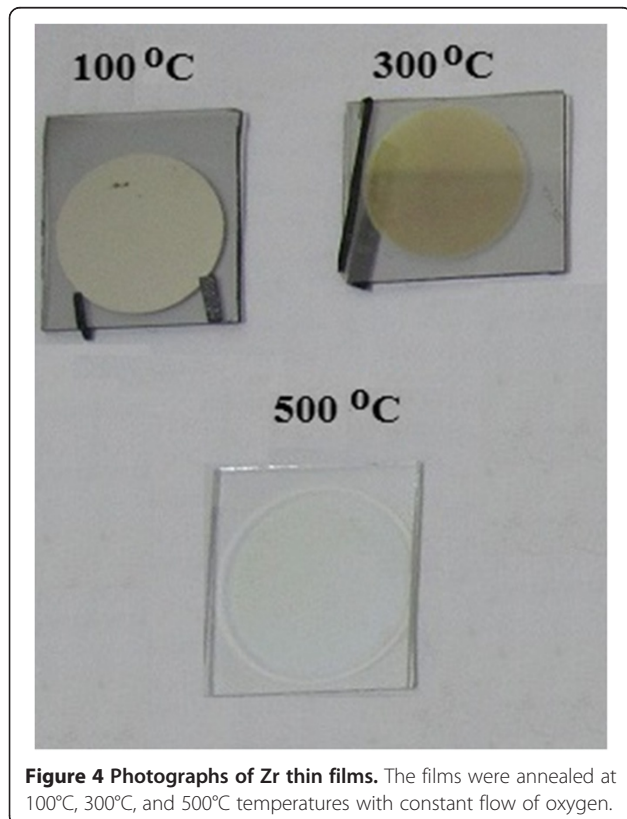
of current as a function of applied voltage and the voltage dependence of electrical resistance of  $ZrO_x$  thin films obtained from Figure 5 data, respectively.

It can be seen that variation of electrical resistance with applied voltage is approximately constant within the experimental error of 10%, for each  $ZrO_x$  sample, while it increases with the annealing temperature. This behavior can be related to the increased oxidation rate as discussed above and is consistent with the EDAX results. When the number of oxygen atoms that should bond to the zirconium atoms is not enough, the remainder Zr atoms act as

donors and can provide free electrons. With these free electrons, the films have a high carrier density and low resistivity. However, as the number of oxygen atoms integrated within the zirconium atoms increases, the number of these free electrons decreases and the film resistance increases.

### Conclusion

A DC magnetron sputtering system was used to deposit Zr thin films of 90-nm thickness on glass substrates. The influence of post-annealing temperature in the presence of constant oxygen flow on crystallographic structure, surface morphology, and chemical composition of the produced samples was studied by XRD, AFM, and EDAX techniques, respectively. A two-probe instrument with an excitation wavelength of 320 nm was employed for electrical resistance investigation. The annealed films at lower temperatures of 100°C and 200°C (group I) had a combined structure of  $ZrO_2$  (orthorhombic) and Zr (hexagonal), while the annealed films at higher temperatures >300°C (group II) were completely oxidized and showed a mixed crystallographic structure of monoclinic



and tetragonal. The crystallite size, nanostrain, and surface roughness were increased with the annealing temperature in each group of the samples. The stoichiometry and color of the zirconium oxide thin films were found to be approximately 1.6 (grey), 1.7 (grey), 1.9 (brown), 2.1 (transparent), and 2.2 (transparent) at annealing temperatures of 100°C, 200°C, 300°C, 400°C, and 500°C, respectively. The variation of electrical resistance of the films was almost constant with applied voltage for each sample. The electrical resistance of  $ZrO_x$  thin films was increased with the annealing temperature.

#### Competing interests

The authors declare that they have no competing interests.

#### Authors' contributions

All authors provided the same contributions in this article. All authors read and approved the final manuscript.

#### Acknowledgements

This work was carried out with the support of the Islamic Azad University, Chalous Branch and Central Tehran Branch. HS acknowledges the University of Tehran and is grateful to the Centre of Excellence for Physics of Structure and Microscopic Properties of Matter, Department of Physics, University of Tehran for partial support of this work.

#### Author details

<sup>1</sup>Department of Physics, Chalous Branch, Islamic Azad University, Chalous, Iran. <sup>2</sup>Department of Physics, University of Tehran, North Kargar Street, Tehran, Iran. <sup>3</sup>Department of Physics, Faculty of Science, Central Tehran Branch, Islamic Azad University, Tehran, Iran.

Received: 2 August 2013 Accepted: 3 October 2013

Published: 20 October 2013

#### References

1. Askeland, DR, Phulé, PP: *The Science and Engineering of Materials*, 4th edn. Thomson Brooks/Cole, Pacific Grove (2003)
2. Gan, Z, Yu, GQ, Zhao, ZW, Tan, CM, Tay, BK: Mechanical properties of zirconia thin films deposited by filtered cathodic vacuum arc. *J. Am. Ceram. Soc.* **88**, 2227–2229 (2005)
3. Martin, PJ, Bendavid, A: Properties of zirconium oxide films prepared by filtered cathodic vacuum arc deposition and pulsed DC substrate bias. *Thin Solid Films* **518**, 5078–5082 (2010)
4. Sui, JH, Cai, W: Formation of  $ZrO_2$  coating on the NiTi alloys for improving their surface properties. *Nucl. Instrum. Methods Phys. Res. B* **251**, 402–406 (2006)
5. Zhao, ZW, Tay, BK, Yu, GQ, Lau, SP: Optical properties of filtered cathodic vacuum arc-deposited zirconium oxide thin films. *J. Phys. Condens. Matter* **15**, 7707–7716 (2003)
6. Yu, GQ, Tay, BK, Zhao, ZW: Structure and properties of zirconium oxide thin films prepared by filtered cathodic vacuum arc. *Appl. Phys. A Mater. Sci. Proc.* **81**, 405–411 (2005)
7. Liu, X, Huang, A, Ding, C, Chu, PK: Enhanced bioactivity of self-organized  $ZrO_2$  nanotube layer by annealing and UV irradiation. *Biomaterials* **27**, 3904–3911 (2006)
8. Ohtsu, Y, Hino, Y, Misawa, T, Fujita, H, Yukimura, K, Akiyama, M: Influence of ion-bombardment-energy on thin zirconium oxide films prepared by dual frequency oxygen plasma sputtering. *Surf. Coat. Technol.* **201**, 6627–6630 (2007)
9. Xu, KW, Zhao, S, Ma, F, Song, ZX: Thickness-dependent structural and optical properties of sputter deposited  $ZrO_2$  films. *Opt. Mater.* **30**, 910–915 (2008)
10. Lai, LJ, Lu, HC, Chen, HK, Cheng, BM, Lin, MI, Chu, TC: Photoluminescence of zirconia films with VUV excitation. *J. Electron. Spectrosc.* **144**, 865–868 (2005)
11. Cyviene, E, Laurikaitis, M, Dudonis, J: Deposition of nanocomposite Zr- $ZrO_2$  films by reactive cathodic vacuum arc evaporation. *Mat. Sci. Eng. B-Solid.* **118**, 238–241 (2005)
12. Korkmaz, S, Pat, S, Ekem, N, Zafer Balbag, M, Temel, S: Thermal treatment effect on the optical properties of  $ZrO_2$  thin films deposited by thermionic vacuum arc. *Vac.* **6**, 1930–1933 (2012)
13. Manicone, PF, Iommetti, PR, Raffaelli, L: An overview of zirconia ceramics: basic properties and clinical applications. *J. Dent.* **35**, 819–826 (2007)
14. Cueto, LF, Sanchez, E, Torres-Martinez, LM, Hirata, GA: On the optical, structural, and morphological properties of  $ZrO_2$  and  $TiO_2$  dip-coated thin films supported on glass substrates. *Mater. Charact.* **55**, 263–267 (2005)
15. Lee, BJ, Sohn, HL, Cho, YT: The effect of the RF-sputtering condition on the  $ZrO_2$  thin film's characteristics. *J. Korean. Phys. Soc.* **51**, 1038–1041 (2007)
16. Shen, YM, Shao, SY, Yu, H, Fan, ZX, He, HB, Shao, JD: Influences of oxygen partial pressure on structure and related properties of  $ZrO_2$  thin films prepared by electron beam evaporation deposition. *Appl. Surf. Sci.* **254**, 552–556 (2007)
17. Huang, AP, Chu, PK: Microstructural improvement of sputtered  $ZrO_2$  thin films by substrate biasing. *Mat. Sci. Eng. B-Solid.* **121**, 244–247 (2005)
18. Huy, LD, Laffez, P, Daniel, P, Jouanneaux, A, Khoi, NT, Simeone, D: Structure and phase component of  $ZrO_2$  thin films studied by Raman spectroscopy and X-ray diffraction. *Mat. Sci. Eng. B-Solid.* **104**, 163–168 (2003)
19. Ehrhart, G, Capoen, B, Robbe, O, Boy, P, Turrell, S, Bouazaoui, M: Structural and optical properties of n-propoxide sol-gel derived  $ZrO_2$  thin films. *Thin Solid Films* **496**, 227–233 (2006)
20. Vrejiu, I, Matei, DG, Morar, M, Epurescu, G, Ferrari, A, Balucani, M, Lamedica, G, Dinescu, G, Grigoriu, C, Dinescu, M: Properties of  $ZrO_2$  thin films prepared by laser ablation. *Mat. Sci. Semicon. Proc.* **5**, 253–257 (2002)
21. Liu, WC, Wu, D, Li, AD, Ling, HQ, Tang, YF, Ming, NB: Annealing and doping effects on structure and optical properties of sol-gel derived  $ZrO_2$  thin films. *Appl. Surf. Sci.* **191**, 181–187 (2002)
22. Zhu, JF, Gao YG, Y, Zhang, LA, Pan, YH, Wang, GD, Xu, Y, Zhang, WH, ZHUJF: Epitaxial growth of ultrathin  $ZrO_2(111)$  films on Pt(111). *Chinese Sci. Bull.* **56**, 502–507 (2011)
23. Ciosek, J, Paszkowicz, W, Pankowski, P, Firak, J, Stanislawek, U, Patron, Z: Modification of zirconium oxide film microstructure during post-deposition annealing. *Vac.* **72**, 135–141 (2004)
24. Kuei, PY, Chou, JD, Huang, CT, Ko, HH, Su, SC: Growth and characterization of zirconium oxide thin films on silicon substrate. *J. Cryst. Growth* **314**, 81–84 (2011)
25. Venkataraj, S, Kappertz, O, Liesch, C, Detemple, R, Jayavel, R, Wutti, M: Thermal stability of sputtered zirconium oxide films. *Vac.* **75**, 7–16 (2004)
26. Chua, DHC, Milne, WI, Zhao, ZW, Tay, BK, Lau, SP, Carney, T, White, RG: Properties of amorphous  $ZrO_x$  thin films deposited by filtered cathodic vacuum arc. *J. Non-Cryst. Solids* **332**, 185–189 (2003)
27. Zhao, ZW, Tay, BK, Huang, L, Yu, GQ: Study of the structure and optical properties of nanocrystalline zirconium oxide thin films deposited at low temperatures. *J. Phys. D Appl. Phys.* **37**, 1701–1705 (2004)
28. Martin, PJ, Netterfield, RP, Sainty, WG: Modification of the optical and structural properties of dielectric  $ZrO_2$  films by ion-assisted deposition. *J. Appl. Phys.* **55**, 235–241 (1984)
29. Mehner, A, Klumper-Westkamp, H, Hoffmann, F, Mayr, P: Crystallization and residual stress formation of sol-gel-derived zirconia films. *Thin Solid Films* **308–309**, 363–368 (1997)
30. Martin, PJ, Netterfiend, RP, Kinder, TJ: Ion-beam-deposited films produced by filtered arcevacaporation. *Thin Solid Films* **193–194**, 77–83 (1990)
31. Pawkewicz, WT, Hays, DD: Microstructure control for sputter-deposited  $ZrO_2$ ,  $ZrO_2$ -CaO and  $ZrO_2$ - $Y_2O_3$ . *Thin Solid Films* **94**, 31–45 (1982)
32. Ochando, IM, Vila, M, Prieto, C: Optical and structural study of EB-PVD  $ZrO_2$  thin films. *Vac.* **81**, 1484–1488 (2007)
33. Haung, AP, Di, ZF, Fu, RKY, Chu, PK: Improvement of interfacial and microstructure properties of high-k  $ZrO_2$  thin films fabricated by filtered cathodic arc deposition using nitrogen incorporation. *Surf. Coat. Technol.* **201**, 8282–8285 (2007)
34. Huang, AP, Fu, RKY, Chu, PK, Wang, L, Cheung, WY, Xu, JB, Wong, SP: Plasma nitridation and microstructure of high-k  $ZrO_2$  thin films fabricated by cathodic arc deposition. *J. Cryst. Growth.* **277**, 422–427 (2005)
35. Savaloni, H, Gholipour-Shahraki, M, Player, MA: A comparison of different methods for x-ray diffraction line broadening analysis of Ti and Ag UHV deposited thin films: nanostructural dependence on substrate temperature and film thickness. *J. Phys. D Appl. Phys.* **39**, 2231–2247 (2006)
36. Chung, FH, Smith, DK: *Industrial Applications of X-ray Diffraction*. Marcel Dekker, New York (1999)

37. Shi, Z, Player, MA: Preferred orientation of evaporated Ni films on Mo and SiO<sub>2</sub> substrates. *Vac.* **49**, 257–263 (1998)
38. Warren, BE: X-Ray Diffraction. Addison Wesley, London (1969)
39. Langford, JI, Wilson, AJ: Scherrer after sixty years: a survey and some new results in the determination of crystallite size: *J. Appl. Cryst.* **11**, 102–113 (1978)
40. Huang, TC, Lim, G, Parmigiani, F, Kay, E: Effect of ion bombardment during deposition on the x-ray microstructure of thin silver films. *J. Vac. Sci. Technol.* **A3**, 2161–2166 (1985)
41. Khojier, K, Savaloni, H, Kangarloo, H, Ghoranneviss, M, Yari, M: Influence of annealing temperature on the nanostructure and corrosivity of Ti/stainless steel substrates. *Appl. Sur. Sci.* **254**, 2528–2533 (2008)
42. Koski, V, HÖlsä, J, Juliet, P: Properties of zirconium oxide thin films deposited by pulsed reactive magnetron sputtering. *Sur. Coat. Technol* **120–121**, 303–312 (1999)

doi:10.1186/2251-7235-7-55

**Cite this article as:** Khojier et al.: Structural, electrical, and decorative properties of sputtered zirconium thin films during post-annealing process. *Journal of Theoretical and Applied Physics* 2013 **7**:55.

**Submit your manuscript to a SpringerOpen<sup>®</sup> journal and benefit from:**

- ▶ Convenient online submission
- ▶ Rigorous peer review
- ▶ Immediate publication on acceptance
- ▶ Open access: articles freely available online
- ▶ High visibility within the field
- ▶ Retaining the copyright to your article

---

Submit your next manuscript at ▶ [springeropen.com](http://springeropen.com)

---